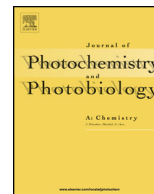Contents lists available at ScienceDirect

Journal of Photochemistry and Photobiology A: Chemistry

journal homepage: www.elsevier.com/locate/jphotochem

Facile fabrication of MoS$_2$/PEDOT–PSS composites as low-cost and efficient counter electrodes for dye-sensitized solar cells

Dandan Song[a], Meicheng Li[a,b,*], Yongjian Jiang[a], Zhao Chen[a], Fan Bai[a], Yingfeng Li[a], Bing Jiang[a]

[a] State Key Laboratory of Alternate Electrical Power System with Renewable Energy Sources, School of Renewable Energy, North China Electric Power University, Beijing 102206, China
[b] Suzhou Institute, North China Electric Power University, Suzhou 215123, China

ARTICLE INFO

ABSTRACT

A novel MoS$_2$/PEDOT–PSS counter electrode (CE) is proposed and used for dye sensitized solar cells (DSCs). The MoS$_2$/PEDOT–PSS composites were facilely obtained from the mechanical mixture of hydrothermal synthesized MoS$_2$ nanomaterial and poly(3,4-ethylenedioxythiophene)–poly(styrenesulfonate) (PEDOT–PSS) aqueous solution, and the composites are compatible to low temperature and cost-effective screen-printing fabrication technique. DSC with MoS$_2$/PEDOT–PSS CE exhibits comparable power conversion efficiency and fill factor to the DSC with conventional Pt CE. The good photovoltaic performance of DSC using MoS$_2$/PEDOT–PSS CE is primarily derived from the high electrocatalytic activity of nanosized MoS$_2$ and the high conductive feature of PEDOT–PSS. These results reveal the potential application of MoS$_2$/PEDOT–PSS composite in the use of low-cost, printable and efficient Pt-free CEs.

© 2014 Elsevier B.V. All rights reserved.

1. Introduction

Dye-sensitized solar cells (DSCs) are potential substitutes for traditional silicon solar cells for their low-cost, high efficiency and flexible applications [1–3]. As one of the most important components in DSC, counter electrode (CE) offers electrons in the reduction process of triiodide [4], which directly influence the photovoltaic properties of DSCs. An ideal CE is supposed to possess several features including high electrocatalytic activity, stable, low cost, and printable (compatible for flexible applications). Platinum (Pt) is the most commonly used CE and exhibits high electrochemical catalytic activity for triiodide reduction [5]. However, it is expensive and probably be corroded in electrolyte [5,6], hampering the scale-up application of DSCs. Therefore, the exploration of Pt-free CE attracts increasing research interests in recent several years [7–9].

Transition metal dichalcogenides (MoS$_2$ in especial), taking the advantages of low cost and inherent material stability (the ability of preventing electrolyte corrosion), are widely used for hydrogen generation [10] and also proved to be active for triiodide reduction

by Wu et al. [11]. Generally, the activity of MoS$_2$ is limited by the population of its active edges, which only constitute a small proportion of the total surface area in the MoS$_2$ film [12,13]. One route to increase the number of active edges is decreasing the size of the MoS$_2$ to nanometer dimension [14,15]. However, MoS$_2$ nanomaterials are prone to stacking together because of its layered nature and the high surface energy of the two dimensional structure, delivering higher resistance for electron transfer and diffusion of reactant molecules, and retarding the catalytic reaction [12,16]. In order to overcome these obstacles, few-layered MoS$_2$ nanocatalysts were deposited on graphene or carbon nanotubes by in situ growth of MoS$_2$ on these supports [16–18]. The obtained composites display significantly enhanced performance for electrocatalytic HER and triiodine reduction. However, the synthesis of these composite materials is complex and the content ratio is hard to control. Hence, it is important to find suitable support and a facile process to construct composites consisting of MoS$_2$ nanocatalysts.

Poly(3,4-ethylenedioxythiophene)–poly(styrenesulfonate) (PEDOT–PSS) is a high conductive polymer and is electrochemical stable in electrolyte which has also been proved to be a good substitute for Pt CE [5,19,20]. In addition, it is easy processing and can form a transparent electrode through screen-printing or spin-coating technique from its aqueous solution followed by a low temperature processing (120 °C for PEDOT–PSS, while typically 450 °C for Pt electrode). Nanomaterials, including carbon black [5], TiN [20], etc., can be well dispersed in PEDOT–PSS solution by simple mechanical mixing. Thereby, PEDOT–PSS is possible to be

* Corresponding author at: State Key Laboratory of Alternate Electrical Power System with Renewable Energy Sources, School of Renewable Energy, North China Electric Power University, Beijing 102206, China. Tel.: +86 10 6177 2951; fax: +86 10 6177 2951.
E-mail addresses: mcli@ncepu.edu.cn, lmc50@cam.ac.uk (M. Li).

an ideal support to avoid the aggregation of MoS_2 nanocatalysts by dispersing MoS_2 in its aqueous solution. Meanwhile, the fabrication of MoS_2/PEDOT–PSS composite electrode will be much facile (such as spin-coating, screen-printing, dip-coating), and as well, the content ratio in the composite can be well controlled by varying the adding content of MoS_2. In addition, the electrochemical stability of MoS_2/PEDOT–PSS composite electrode in electrolyte will be sufficiently good due to the good stability of raw materials. Moreover, the charge transport in the composite film may also be improved as the high conductive PEDOT–PSS chains can provide preferential and continuous charge transport pathways.

Hence, in this work, MoS_2/PEDOT–PSS nanocomposite is fabricated and employed as CE material in DSCs. MoS_2 nanomaterials were synthesized through hydrothermal synthesis and then dispersed in PEDOT–PSS solution through mechanical mixing to form the composite material. The photovoltaic performance of DSCs with this composite CE was characterized, and the electrochemical catalytic mechanism of MoS_2/PEDOT–PSS CE was studied with electrochemical impedance spectroscopy.

2. Experimental

2.1. Materials and synthesis of MoS₂ nanocatalysts

TiO_2 nanoparticles (P25) and N719 dye (Ru(dcbpy)$_2$ (NCS)$_2$(dcbpy = 2,2-bipyridyl-4,4-dicarboxylato)) were purchased from Degussa and Dyesol, respectively. PEDOT–PSS aqueous solution (1.0–1.3 wt% dispersion in water) was obtained from Clevios. The iodide/triiodide liquid electrolyte (DHS-E23), Pt/FTO counter electrode (FTO glass, 15 Ω/sq) and FTO glasses (15 Ω/sq) were acquired from Dalian HeptaChroma SolarTech Co., Ltd. Molybdenum trioxide (MoO_3, AR), sodium sulfide (Na_2S, AR), hydrochloric acid (HCl, AR) and Cetyltrimethyl Ammonium Bromide (CTAB) were purchased from Sinopharm Chemical Reagent Beijing Co., Ltd.

MoS_2 materials were synthesized referring to Ref. [15] by hydrothermal method but using an improved procedure. MoO_3 (0.504 g, 3.5 mmol) and $Na_2S \cdot 9H_2O$ (2.52 g, 10.5 mmol) were added to 35 ml of 0.2 mol/L HCl aqueous solution in a 50 ml Teflon® lined autoclave reactor. Then the mixed solutions were stirred for a good dispersion before being putted into an oven. The reaction carried out at 200 °C for 12 h. The black powder product was centrifuged and washed with distilled water for three times, and dried at 80 °C in vacuum. The related resultant was marked as M1. To control the size of resultant and obtain a small sized MoS_2, CTAB surfactant was introduced to the mixed solution of MoO_3 (0.1 mol/L), $Na_2S \cdot 9H_2O$ (0.3 mol/L) and HCl (0.6 mol/L), and its concentration was 0.02 mol/L. Other preparation procedures were same to these used in the fabrication of M1, and the resultant with CTAB assisted in reaction process was marked as M2.

2.2. Preparation of MoS₂/PEDOT–PSS composite counter electrode and DSCs

MoS_2/PEDOT–PSS nanocomposites were prepared by dispersing MoS_2 powder in PEDOT–PSS aqueous solution, and then stirred and sonicated for several hours to form a well dispersed solution. The counter electrodes (MoS_2/PEDOT–PSS, pristine PEDOT–PSS) were fabricated by spin-coating of their solutions on ozone-treated FTO-glass followed by the drying process at 120 °C in air for 30 min. Dye-sensitized TiO_2 film was prepared by doctor-blading of TiO_2 slurry on a FTO glass and calcinated at 450 °C for 30 min. After cooled to 80 °C, the TiO_2 film was immersed in 0.3 mmol/L ethanol solution of N719 dye for 24 h. Then the dye-sensitized TiO_2 film was washed with anhydrous ethanol and dried

in moisture-free air. Finally, the dye-sensitized TiO_2 photoanode and the as-fabricated CEs were assembled together with 60 μm thick Surlyn. The iodide/triiodide liquid electrolyte with acetonitrile as the solvent was then injected between the two electrodes.

2.3. Characterization methods

The structure and morphology of the materials were characterized by transmission electron microscopy (TEM, FEI Tecnai F20) and scanning electron microscopy (SEM, Hitachi S-4800). The current density–voltage (J–V) characteristics of DSCs were measured with a Keithley 2400 source meter under 100 mW/cm^2 irradiation from a solar simulator (XES-301S + EL-100). The electrochemical impedance spectroscopy (EIS) was carried out using the electrochemical workstation (CHI660D), performed on DSCs under 100 mW/cm^2 irradiation. The frequency range varied from 100 kHz to 0.1 Hz.

3. Results and discussions

3.1. Morphology study of MoS₂ materials and MoS₂/PEDOT–PSS composite electrodes

Fig. 1 shows the structural features of as-fabricated MoS_2 materials (M1 and M2), characterized by TEM and SEM measurements. From the TEM image of M1 shown in Fig. 1(a), it can be seen that M1 is composited by the nanosheets which aggregate obviously though after the ultrasonic treatment in ethanol before TEM measurement. SEM image in Fig. 1(b) presents the bulk structure of M1 powder, which consists of large solid aggregates with size of several tens to hundreds of nanometers. With CTAB surfactant in the preparing process, the size of the resultant has been reduced as expected, i.e., M2 exhibits nanoflake structure with a size of 30–40 nm as shown by TEM image in Fig. 1(d). The powder of M2 also possesses a small size than that of M1 (as shown by SEM images in Fig. 1(e)), and is supposed to be more efficient when used as electrocatalytic active sites. The high resolution TEM (HRTEM) images in Fig. 1(c) and (f) reveal the crystalline nature of these two MoS_2 materials, which display the typical lattice fringes at the edge of multi-layered crystalline MoS_2.

Fig. 2 shows the film feature of MoS_2/PEDOT–PSS nanocomposite electrodes fabricated by spin-coating of the mechanical mixture of MoS_2 powders and PEDOT–PSS aqueous solution, characterized by SEM technique. It can be found that in both cases, M1 or M2 doped PEDOT–PSS, MoS_2 materials are well dispersed. The particles in M1/PEDOT–PSS are much smaller than M1 powders (Fig. 2(a)), indicating that the aggregation of MoS_2 materials is able to be suppressed in some extent through dispersing into PEDOT–PSS. Furthermore, these two composite electrodes are porous with multiple interspaces, which are expected to possess large effective electrochemical surfaces and are considered to be crucial for high electrocatalytic activity [19].

3.2. Photovoltaic performance of DSCs with MoS₂/PEDOT–PSS composite counter electrodes

The photocurrent density–voltage (J–V) curves of DSCs with different CEs are shown in Fig. 3(a), and the photovoltaic (PV) parameters are listed in Table 1. The photoelectric conversion efficiency (PCE) and fill factor (FF) of DSC using M2/PEDOT–PSS CE are higher than these of DSC using M1/PEDOT–PSS CE, which are 5.7% and 0.58 for the former while 4.7% and 0.50 for the latter, respectively. The differences in PV performance of the DSCs using these two different CEs prove that MoS_2 material with small size is more efficient for the use of CE materials. Nevertheless, both composite CEs present better performance than pristine PEDOT–PSS CE. As
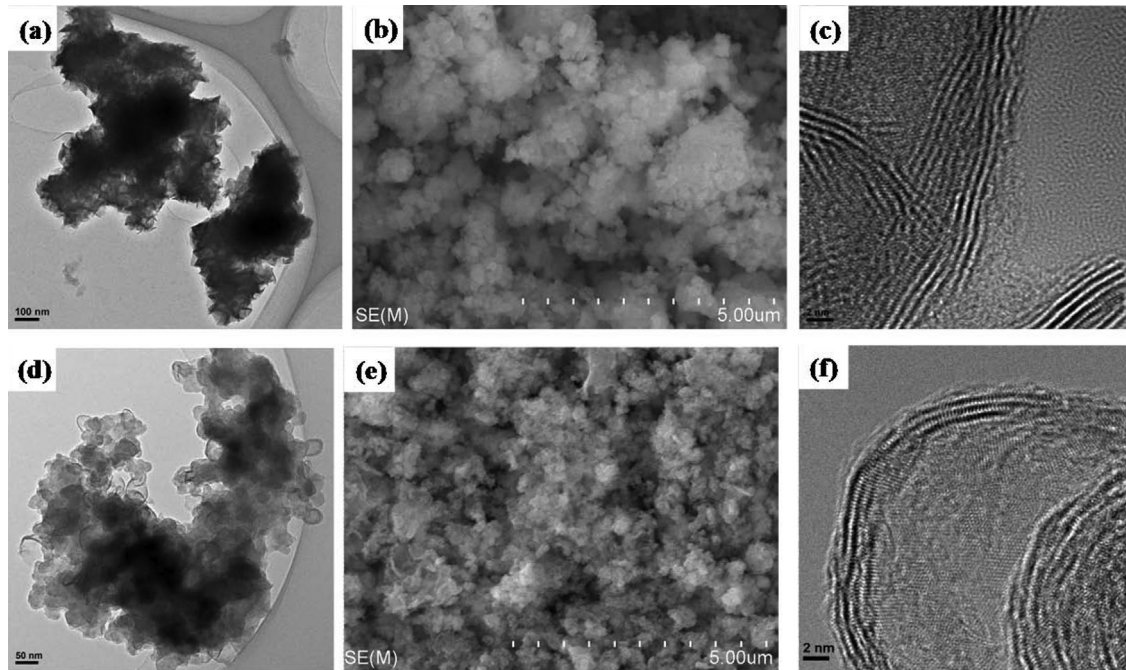
D. Song et al. / Journal of Photochemistry and Photobiology A: Chemistry 279 (2014) 47–51   49

Fig. 1. TEM, SEM and HRTEM images of M1 (a, b, c) and M2 (d, e, f), respectively.
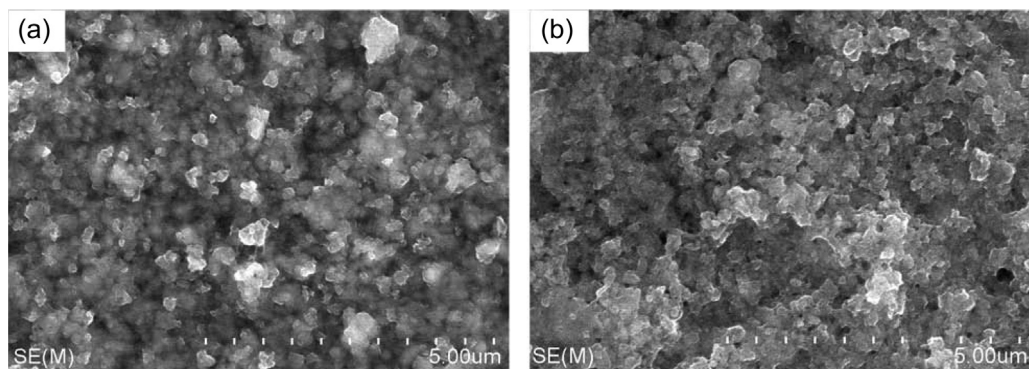

Fig. 2. SEM images from M1 doped PEDOT–PSS film (a) and M2 doped PEDOT–PSS film (b), respectively.

can be seen from Fig. 3(a) and Table 1, DSC with PEDOT–PSS CE yields much lower FF and PCE, as also observed in previous literatures [5,19,20]. The DSC using standard Pt CE was also fabricated, and it performs a higher V_{OC} than PEDOT–PSS based CEs due to the lower overpotential needed in driving the reduction of triiodide in CE. When comparing the DSC with M2/PEDOT–PSS CE with the one utilizing conventional Pt CE, it can be found that these two DSCs exhibit comparable PV performance with similar fill factors and shapes of *J*–*V* curves. Though the PCE of DSC with M2/PEDOT–PSS CE is a bit lower, it can be improved by systematic experimental optimization. As illustrated by Fig. 3(b), by simply varying the doping content of MoS_2 in PEDOT–PSS matrix and the spin-coating speed during film fabrication, the PV performance of DSCs presents significant changes. For example, when using the conditions of 50 mg
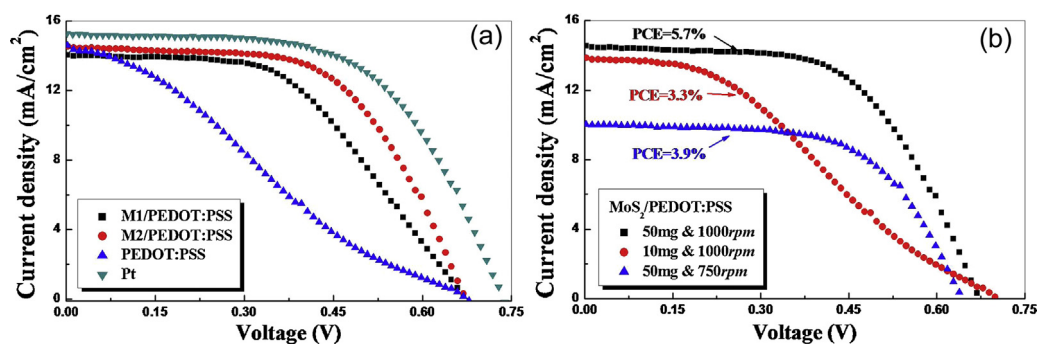

Fig. 3. The current density–voltage characteristics of DSCs using various counter electrodes (a), and using MoS_2/PEDOT–PSS CEs with different MoS_2 dosage and spin-coating speeds during fabrication (b).

Table 1
Photovoltaic performance of DSCs using different counter electrodes.

CEs	J_{SC} (mA/cm^2)	V_{OC} (V)	PCE (%)	FF
M1/PEDOT–PSS	14.0	0.68	4.7	0.50
M2/PEDOT–PSS	14.55	0.68	5.7	0.58
PEDOT–PSS	14.6	0.68	2.5	0.26
Pt	15.26	0.73	6.6	0.59

MoS_2 (M2) doped in PEDOT–PSS matrix and a spin-coating speed of 1000 rpm (marked as (50 mg and 1000 rpm) for abbreviation) for fabricating MoS_2/PEDOT–PSS CE, the PCE of corresponding DSC is 1.7 times higher than that of DSC with the CE fabricated under the conditions of (10 mg and 1000 rpm). Hence, it can be expected that the PV performance of DSC with M2/PEDOT–PSS CE can be further improved by further optimization of these experimental parameters, and is potential to be even better than that of DSC with conventional Pt CE. Hence, these results prove that M2/PEDOT–PSS CE is potential to be used as a substitute for Pt CE.

3.3. The electrochemical catalytic mechanism of MoS_2/PEDOT–PSS composite CE

Generally, the effect of CE on PV performance is ascribed to the kinetic features of the electrochemical process. To get an insight in the electrochemical catalytic mechanism of MoS_2/PEDOT–PSS composite CE, electrochemical impedance spectroscopy (EIS) is employed. Fig. 4 shows the Nyquist plots from DSCs utilizing Pt, PEDOT–PSS and MoS_2 (M2)/PEDOT–PSS CEs, all of which contain the typical three semicircles relating to the three kinetic stages of the electrochemical reaction process. Fig. 4 inset shows the equivalent circuit of a DSC, in which R_S, R_{ct1} and R_{ct2} represent for the series resistance at electrode/FTO interface, the charge transfer resistance at electrolyte/CE interface and the charge transfer resistance at TiO_2/electrolyte interface, and Z_N represents for the Nernst diffusion resistance of redox couple in the electrolyte [21,22]. Z_{diff} reflects the porous diffusion impedance of redox couple in the porous CE, which is only involved in the CE with large active areas and in responses in the mid-frequency region of the Nyquist plot [22]. The values of these components are simulated by fitting the experimental spectra with the equivalent circuit. The simulated R_S values for MoS_2/PEDOT–PSS CE is 13.5 Ω and for Pt CE is 23.1 Ω. The small R_S indicates that MoS_2/PEDOT–PSS is well bonded to the FTO surface. As R_S from pure MoS_2 CE is usually higher than that of Pt CE [11,18], the lower value from MoS_2/PEDOT–PSS CE can be ascribed to the effect of PEDOT–PSS, which acts as a binder and improves the binding of MoS_2 to the FTO glass substrate. Indeed, the R_S from pristine PEDOT–PSS electrode is also low (13.1 Ω). The R_{ct1} from

MoS_2/PEDOT–PSS and Pt CEs are 8.9 Ω and 10.3 Ω, respectively, indicating the comparable electrochemical catalytic performance of these two electrodes on triiodide reduction. In addition, the total impedance differs little in DSCs employing MoS_2/PEDOT–PSS or Pt CEs, in accordance with the comparable PV performance of corresponding DSCs. Moreover, the component Z_{diff} associating with porous CEs has been significantly decreased in MoS_2/PEDOT–PSS CE compared to PEDOT–PSS CE, i.e., 4.6 Ω for the former while 51.0 Ω for the latter, implying an improved catalytic kinetic inner the CEs. From EIS results, it is further proved that the MoS_2/PEDOT–PSS CE possesses excellent catalytic activity of triiodide reduction.

As MoS_2 has an intrinsic higher electrocatalytic activity as compared with PEDOT–PSS, when the MoS_2 nanoflakes doped with PEDOT–PSS, they will act as high active sites and have a dominant advantage over PEDOT–PSS to catalytic the reduction of triiodide to iodide. On the other hand, PEDOT–PSS can improve the interface contact of FTO/CE which facilitates electron transfer at FTO/CE interface. In addition, PEDOT–PSS chains may provide efficient carrier transport paths due to its high electrical conductivity property. Hence, the MoS_2/PEDOT–PSS electrode performs synergetic effect on triiodide reduction and exhibits the Pt-like electrocatalytic feature.
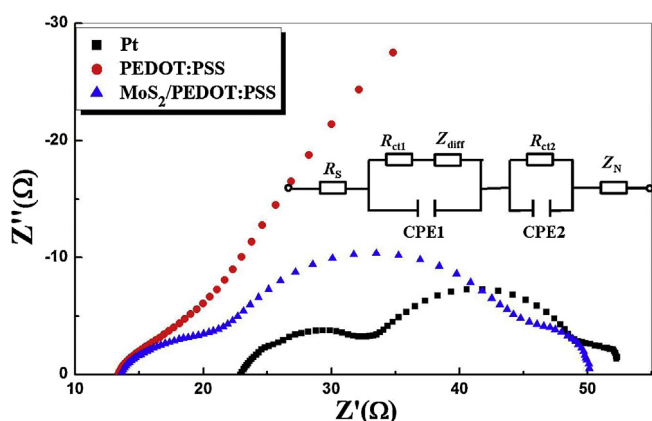
4. Conclusions

The novel inorganic/organic nanocomposite composed of MoS_2 nanoflakes and PEDOT–PSS was obtained through simple mechanical dispersion of MoS_2 powders in aqueous PEDOT–PSS solution. Employing this composite as a counter electrode, the DSC exhibits comparable photovoltaic performance with the one using Pt counter electrode. The good photovoltaic performance of DSC with MoS_2/PEDOT–PSS counter electrode results from the Pt-like electrocatalytic property of MoS_2/PEDOT–PSS, deriving from the combination effect of MoS_2 and PEDOT–PSS, i.e., MoS_2 acts as active sites for the triiodide reduction and PEDOT–PSS improves the electrical performance. This work proves that MoS_2/PEDOT–PSS composite is potential for the use of low-cost, printable and efficient Pt-free counter electrode materials.

Fig. 4. Nyquist plots from DSCs using different counter electrodes under 100 mW/cm^2. Inset shows the equivalent circuit of DSCs.

References

[1] M. Grätzel, Recent advances in sensitized mesoscopic solar cells, Accounts of Chemical Research 42 (2009) 1788–1798.
[2] S. Park, H. Jung, B. Kim, W. Lee, MWCNT/mesoporous carbon nanofibers composites prepared by electrospinning and silica template as counter electrodes for dye-sensitized solar cells, Journal of Photochemistry and Photobiology A: Chemistry 246 (2012) 45–49.
[3] B.E. Hardin, H.J. Snaith, M.D. McGehee, The renaissance of dye-sensitized solar cells, Nature Photonics 6 (2012) 162–169.
[4] A. Kay, M. Grätzel, Low cost photovoltaic modules based on dye sensitized nanocrystalline titanium dioxide and carbon powder, Solar Energy Materials & Solar Cells 44 (1996) 99–117.
[5] P. Balraju, P. Suresh, M. Kumarb, M.S. Roy, G.D. Sharma, Effect of counter electrode, thickness and sintering temperature of TiO2 electrode and TBP addition in electrolyte on photovoltaic performance of dye sensitized solar cell using pyronine G (PYR) dye, Journal of Photochemistry and Photobiology A: Chemistry 206 (2009) 53–63.

[6] G. Syrrokostas, A. Siokou, G. Leftheriotis, P. Yianoulis, Degradation mechanisms of Pt counter electrodes for dye sensitized solar cells, Solar Energy Materials & Solar Cells 103 (2012) 119–127.

[7] S. Peng, Y. Wu, P. Zhu, V. Thavasi, S.G. Mhaisalkar, S. Ramakrishn, Facile fabrication of polypyrrole/functionalized multiwalled carbon nanotubes composite as counter electrodes in low-cost dye-sensitized solar cells, Journal of Photochemistry and Photobiology A: Chemistry 223 (2011) 97–102.

[8] M. Wu, X. Lin, Y. Wang, L. Wang, W. Guo, D. Qi, X. Peng, A. Hagfeldt, M. Grätzel, T. Ma, Economical Pt-free catalysts for counter electrodes of dye-sensitized solar cells, Journal of the American Chemical Society 134 (2012) 3419–3428.

[9] Y. Hou, D. Wang, X.H. Yang, W.Q. Fang, B. Zhang, H.F. Wang, G.Z. Lu, P. Hu, H.J. Zhao, H.G. Yang, Rational screening low-cost counter electrodes for dye-sensitized solar cells, Nature Communications 4 (2013) 1583.

[10] A.B. Laursen, S. Kegnæs, S. Dahl, I. Chorkendorff, Molybdenum sulfides-efficient and viable materials for electro- and photoelectrocatalytic hydrogen evolution, Energy & Environmental Science 5 (2012) 5577.

[11] M. Wu, Y. Wang, X. Lin, N. Yu, L. Wang, A. Hagfeldt, T. Ma, Economical and effective sulfide catalysts for dye-sensitized solar cells as counter electrodes, Physical Chemistry Chemical Physics 13 (2011) 19298–19301.

[12] T.F. Jaramillo, K.P. Jørgensen, J. Bonde, J.H. Nielsen, S. Horch, I. Chorkendorff, Identification of active edge sites for electrochemical H_2 evolution from MoS_2 nanocatalysts, Science 317 (2007) 100.

[13] V.W. Lau, A.F. Masters, A.M. Bond, T. Maschmeyer, Ionic-liquid-mediated active-site control of MoS_2 for the electrocatalytic hydrogen evolution reaction, Chemistry – A European Journal 18 (2012) 8230–8239.

[14] S. Wang, C. An, J. Yuan, Synthetic fabrication of nanoscale MoS_2-based transition metal sulfides, Materials 3 (2010) 401–433.

[15] W. Li, E. Shi, J. Ko, Z. Chen, H. Ogino, T. Fukud, Hydrothermal synthesis of MoS_2 nanowires, Journal of Crystal Growth 250 (2003) 418–422.

[16] S. Min, G. Lu, Sites for high efficient photocatalytic hydrogen evolution on a limited-layered MoS_2 cocatalyst confined on graphene sheets – the role of graphene, The Journal of Physical Chemistry C 116 (2012) 25415–25424.

[17] G. Yue, J. Lin, S. Tai, Y. Xiao, J. Wu, A catalytic composite film of MoS_2/graphene flake as a counter electrode for Pt-free dye-sensitized solar cells, Electrochimica Acta 85 (2012) 162–168.

[18] S. Tai, C. Liu, S. Chou, S. Chien, J. Lin, T. Lin, Few-layer MoS_2 nanosheets coated onto multi-walled carbon nanotubes as a low-cost and highly electrocatalytic counter electrode for dye-sensitized solar cells, Journal of Materials Chemistry 22 (2012) 24753.

[19] J. Chen, H. Wei, K. Ho, Using modified poly(3,4-ethylene dioxythiophene):poly(styrenesulfonate) film as a counter electrode in dye-sensitized solar cells, Solar Energy Materials & Solar Cells 91 (2007) 1472–1477.

[20] H. Xu, X. Zhang, C. Zhang, Z. Liu, X. Zhou, S. Pang, X. Chen, S. Dong, Z. Zhang, L. Zhang, P. Han, X. Wang, G. Cui, Nanostructured titanium nitride/PEDOT:PSS composite films as counter electrodes of dye-sensitized solar cells, ACS Applied Materials & Interfaces 4 (2012) 1087–1092.

[21] J.D. Roy-Mayhew, D.J. Bozym, C. Punckt, I.A. Aksay, Functionalized graphene as a catalytic counter electrode in dye-sensitized solar cells, ACS Nano 4 (2010) 6203–6211.

[22] Q. Wang, J.E. Moser, M. Grätzel, Electrochemical impedance spectroscopic analysis of dye-sensitized solar cells, The Journal of Physical Chemistry B 109 (2005) 14945–14953.